Is it really naked? On cosmic censorship in string theory

Andrei V. Frolov*
KIPAC/SITP, Stanford University Stanford, California, 94305-4060 USA
(Received 13 September 2004; published 18 November 2004)

We investigate the possibility of cosmic censorship violation in string theory using a characteristic double-null code, which penetrates horizons and is capable of resolving the spacetime all the way to the singularity. We perform high-resolution numerical simulations of the evolution of negative mass initial scalar field profiles, which were argued to provide a counterexample to cosmic censorship conjecture for AdS-asymptotic spacetimes in five-dimensional supergravity. In no instances formation of naked singularity is seen. Instead, numerical evidence indicates that black holes form in the collapse. Our results are consistent with earlier numerical studies, and explicitly show where the 'no black hole' argument breaks.

DOI: 10.1103/PhysRevD.70.104023 PACS numbers: 04.20.Dw, 04.25.Dm, 04.65.+e

I. INTRODUCTION

Cosmic censorship conjecture remains an unsolved problem in general relativity. In the absence of proof, finding an acceptable counterexample is very important, as it would resolve the issue one way or the other. But even that remains elusive. While there are numerous examples of initial conditions that form a naked singularity in general relativity, none of them are generic as required by the terms of the cosmic censorship conjecture.

Recently, Hertog, Horowitz, and Maeda argued that cosmic censorship is generically violated in asymptotically anti de Sitter spacetimes [1], particularly in five-dimensional supergravity arising from string theory constructs [2]. The counterexample consists of an initial data set which is known to form a singularity and an argument that it cannot form a black hole in the collapse. That would leave the possibilities that singularity is naked, which would disprove cosmic censorship conjecture, or consumes the entire spacetime (big crunch), which initially was deemed unlikely by the authors.

These papers have caused quite a controversy in the literature. The arguments of [1,2] were called into question by a number of papers, on grounds of both analytical [3,4] and numerical [5–7] calculations. The authors themselves pointed out a gap [8] in their first example [1], and reconsidered the possibility of a big crunch [9].

The present paper investigates the possibility of cosmic censorship violation numerically. Earlier numerical studies [5–7] are suggestive of a black hole formation. However, they are not conclusive due to the flawed coordinate choice, which breaks at the moment of apparent horizon formation, and prevents the code from seeing the whole spacetime, thus leaving the possibility of a singularity subsequently becoming naked. This shortcoming is resolved in the present paper by using a characteristic double-null code.

*Electronic address: afrolov@stanford.edu

Conceptually, the code is similar to the one used to investigate the global structure of the spacetime in the critical collapse of the scalar field [10], although the implementation is entirely new. Several issues specific to asymptotically AdS spacetimes had to be addressed, particularly, boundary conditions at infinity.

We focus on cosmic censorship counterexample in the string theory context [2], and perform high-resolution numerical simulations of the evolution of two families of negative mass initial scalar field profiles for various values of parameters and different boundary conditions at the cut-off. In no instances formation of naked singularity is seen. Instead, numerical evidence indicates that black holes form in the collapse, in agreement with [5]. Our results clearly show where the "no black hole" argument of [2] fails.

The paper is organized as follows: In Sec. II, the issue of a coordinate choice is discussed in view of the requirements of testing cosmic censorship conjecture numerically. The scalar field evolution equations and the implementation of the algorithm are described in Sec. III. The numerical results of investigation of cosmic censorship in string theory are given in Sec. IV, and summarized in Sec. V.

II. COORDINATE CHOICE

In numerical investigations of singularity formation and global structure of the spacetime, the coordinate choice plays a crucial role. To study the global structure, coordinates must cover the entire spacetime. To see the singularity inside a black hole, coordinates must penetrate the horizon. To prevent the singularity from corrupting the rest of the spacetime once it forms (if it is not naked, that is), the information propagation speed (both numerical and true characteristic) must be under control. These issues cannot be avoided if one wishes to study cosmic censorship numerically.

In this paper, we adopt double-null coordinate system, which is particularly suited for the above requirements. The spherically symmetric $(n+2)$-dimensional spacetime metric can be written as

$$ds^2 = e^{-2\sigma} d\eta^2 + r^2 d\Omega_n^2, \tag{1}$$

where $d\Omega_n^2$ is the metric of a unit n-dimensional sphere, and the two-manifold metric $d\gamma^2 = e^{-2\sigma} d\eta^2$ is written in explicitly conformally-flat form. Throughout the paper, we will be freely switching between Minkowski and double-null coordinates on the flat two-manifold

$$d\eta^2 = -dt^2 + dx^2 = -4 du dv, \tag{2}$$

with $u = (t-x)/2$ and $v = (t+x)/2$. The familiar form of anti de Sitter metric in spherically symmetric static coordinates

$$ds^2 = -\left(1 + \frac{r^2}{\ell^2}\right) dt^2 + \frac{dr^2}{1 + \frac{r^2}{\ell^2}} + r^2 d\Omega_n^2 \tag{3}$$

transforms to

$$r = \ell \tan\frac{x}{\ell}, \sigma = \ln\left(\cos\frac{x}{\ell}\right) \tag{4}$$

in coordinate system (1). One should note that the peculiar property of AdS that the spatial infinity 'is not very far away' is reflected in the fact that a finite interval $x \in [0, \frac{\pi}{2}\ell]$ covers the whole AdS spacetime in conformal coordinates (1). Indeed, these are the coordinates used in construction of a Carter-Penrose conformal diagram of the AdS spacetime.

In spherical symmetry, one can define a local mass by

$$f \equiv g^{\mu\nu} r_{,\mu} r_{,\nu} = 1 - \frac{2m}{r^{n-1}}. \tag{5}$$

The function f carries information about the spacetime structure: it is negative in the trapped (or antitrapped) region, positive in the regular region, and vanishes on the apparent horizon. The mass function defined by (5) coincides with ADM mass in asymptotically flat spacetimes. In asymptotically AdS spacetimes, however, it diverges near spatial infinity. The physical cause for this is simple: AdS has a constant (negative) energy density while the volume is infinite. To avoid infinities, one can subtract the divergent part from the definition of the mass

$$\mu = m + \frac{1}{2}\frac{r^{n+1}}{\ell^2}, \tag{6}$$

where ℓ is the curvature radius of the asymptotic AdS. We will refer to this mass definition as the *reduced mass*.

Although traditionally used in numerical relativity, Schwarzschild coordinates, like the ones in metric (3), are not suited to study the possible violation of cosmic censorship in dynamical evolution. They do not penetrate horizons (at the apparent horizon, $f = g^{rr} = 0$, so the metric coefficient g_{rr} necessarily diverges), and therefore have no chance of seeing, for example, the destruction of a black hole by infall of a negative mass and 'baring' of the singularity inside (if it actually happens). Unfortunately, Schwarzschild coordinates were the coordinates used in recent numerical studies [5–7] of the possible counterexamples to cosmic censorship in asymptotically AdS spacetimes [1,2]. Although the formation of a trapped surface is seen, the further fate of the spacetime remains unknown. This renders the results of [5–7] largely inconclusive as far as the possible violation of the cosmic censorship goes.

There are coordinate systems other than (1) which do penetrate the horizon, most notably the ingoing Eddington-Finkelstein coordinates

$$ds^2 = -f e^{2g} dv^2 + 2 e^g dv dr + r^2 d\Omega_n^2. \tag{7}$$

However, in implementation of the evolution code based on this coordinate system (which we did as well, although it is not going to be further discussed in this paper) one encounters a problem that the numerical information propagation speed is *higher* than the true speed of the outgoing characteristic (which varies on the grid). This leads to termination of the numerical evolution in the regions causally disconnected from the singularity, which is not a satisfactory behavior for a code that aspires to resolve the global structure of the spacetime.

The true strength of double-null coordinate system (1) is the advantage of knowing the speed of information propagation *everywhere in advance*. The importance of this point cannot be overemphasized, as numerical information propagation properties is what makes or breaks the numerical code which has to deal with singularities before any other factor even comes into play.

The final issue that needs to be discussed before we go over to evolution equations is the gauge choice. The form of the metric (1) is left invariant under rescaling of null coordinates

$$u \mapsto U(u), \qquad v \mapsto V(v). \tag{8}$$

We use this gauge freedom to place initial and boundary surfaces at known coordinate locations, namely, fix center of spacetime and constant-r cut-off at $x = 0$ and $x = c$ correspondingly, and put initial data surface at $t = 0$ timeslice, as illustrated in Fig. 1. This can always be achieved simply by putting $u = v$ at $r = 0$ and $u = -v$ at initial surface, while rescaling v to have $v - u = c$ at cut-off. In fact, it does not even fix the gauge uniquely. The residual gauge freedom (8) is determined by

$$V(u) - U(u) = 0, \qquad u > 0, \tag{9a}$$

$$V(u + c) - U(u) = c, \qquad u > -c, \tag{9b}$$

$$V(-u) + U(u) = 0, \qquad 0 \geq u \geq -c, \tag{9c}$$

and amounts to an odd periodic function ω of period c, with $V(u) = U(u) = u + \omega(u)$.

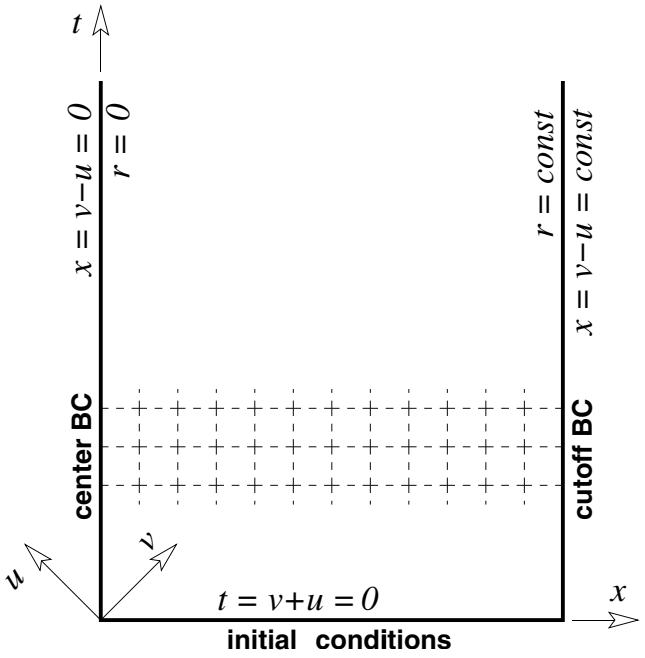

FIG. 1. Coordinate choice.

III. SCALAR FIELD EVOLUTION

The dynamics of a scalar field ϕ with potential $V(\phi)$ minimally coupled to gravity in $N = 2 + n$ dimensions is described by the action

$$S = \frac{1}{16\pi G}\int\{R - g^{\mu\nu}\phi_{,\mu}\phi_{,\nu} - 2V(\phi)\}\sqrt{-g}d^N x. \quad (10)$$

Spherical symmetry effectively reduces the problem to evolution of three nonlinearly coupled scalar fields on a flat two-dimensional manifold. Substituting the spherically symmetric metric (1) into the scalar field action (10) and integrating over the n-dimensional spherical subspace, one obtains the reduced action

$$S \propto \int\left\{\frac{n(n-1)}{r^2}[(\nabla r)^2 + e^{-2\sigma}] - \frac{2n}{r}(\nabla r\cdot\nabla\sigma) - (\nabla\phi)^2 - 2e^{-2\sigma}V(\phi)\right\}r^n d^2x, \quad (11)$$

which describes the dynamics of a spherically symmetric gravitating scalar field. Here and later the differential operators (gradient ∇ and D'Alembertian $\Box$) are taken with respect to the flat two-dimensional metric (2). Variation of the reduced action with respect to field variables σ, ϕ, and r gives equations of motion

$$\frac{r\Box r}{n-1} + (\nabla r)^2 = e^{-2\sigma}\left(1 - \frac{2r^2V}{n(n-1)}\right), \quad (12a)$$

$$\Box\phi + \frac{n}{r}(\nabla r\cdot\nabla\phi) = e^{-2\sigma}V', \quad (12b)$$

$$\Box\sigma - \frac{n}{2}\frac{\Box r}{r} - \frac{1}{2}(\nabla\phi)^2 = \frac{2}{n}e^{-2\sigma}V, \quad (12c)$$

while constraint equations

$$\text{Traceless}\left[r_{,ab} + 2r_{(,a}\sigma_{,b)} + \frac{r}{n}\phi_{,a}\phi_{,b}\right] = 0 \quad (13)$$

are recovered by variation with respect to the (flat) two-metric η_{ab}. The traceless part of a symmetric two-tensor has two independent components, which means there are two constraints. They can be taken either as $\{uu\}$ and $\{vv\}$ or $\{xt\}$ and $\{xx\} + \{tt\}$ components of (13).

The evolution code uses a semiconstrained algorithm. Rather than solve dynamical Eq. (12c) directly, ingoing (uu) null constraint equation

$$r_{,uu} + 2r_{,u}\sigma_{,u} + \frac{r}{n}\phi_{,u}^2 = 0 \quad (14)$$

is integrated to obtain one of the metric coefficients. The integration is particularly easy to do if one defines a new field variable

$$g = -2\sigma - \ln(-r_{,u}), \quad (15)$$

in terms of which the constraint (14) is written simply as

$$g_{,u} = \frac{r}{n}\frac{\phi_{,u}^2}{r_{,u}}. \quad (16)$$

The field variable g actually has a meaning beyond a mere computational convenience. It is the same g which enters coefficients of the Eddington-Finkelstein metric (7).

Equation (12a) warrants further discussion. It involves a delicate cancellation of terms in both small r and large r regimes, which makes it susceptible to discretization errors. The loss of precision can be catastrophic, leading to numerical instability developing at either $r = 0$ or large r and subsequent code failure. After trying various discretization schemes, we settled on discretizing a form of Eq. (12a) which eliminates nonlinear gradient term in favor of a box operator for small r

$$\frac{\Box(r^n)}{n(n-1)} = -r^{n-2}r_{,u}e^g\left(1 - \frac{2r^2V}{n(n-1)}\right), \quad (17)$$

while for large r, the Eq. (12a) rewritten in terms of inverse radius $\rho = 1/r$ is discretized instead

$$\rho\Box\rho - (n+1)(\nabla\rho)^2 = -\rho_{,u}e^g\left[(n-1)\rho^2 - \frac{2}{n}V\right]. \quad (18)$$

This largely circumvents the stability problems mentioned, while still being possible to discretize efficiently.

The Cauchy problem for evolution equations (12) requires specification of six functions of one variable at the initial spacelike surface: the values of three fields r, σ, ϕ and their time derivatives $\dot{r}$, $\dot{\sigma}$, $\dot{\phi}$. These six functions are not independent in general relativity; they must satisfy two constraint equations (13). We restrict our attention to time-symmetric initial data. In covariant form, the requirement of time symmetry is written as

$$\mathcal{K}_{ab} = 0, \qquad \boldsymbol{n} \cdot \nabla \phi = 0, \tag{19}$$

where $\mathcal{K}_{ab}$ is an extrinsic curvature and $\boldsymbol{n}$ is the normal to the initial data surface. In our gauge, the initial surface is $t = 0$, so the condition of time symmetry is simply that the time derivatives $\dot{r}$, $\dot{\sigma}$, $\dot{\phi}$ vanish. This requirement satisfies the $\{tx\}$ constraint identically, which leaves three functions subject to one constraint for specification of the initial data. Of the two freely specifiable functions, one is physical—the initial scalar field profile, and the other is a gauge choice fixing residual gauge freedom (9).

Once the scalar field profile is specified on the initial time slice, the rest of the variables are obtained by integrating

$$r_{,x} = \left(1 - \frac{2m}{r^{n-1}}\right) e^{g}, \tag{20a}$$

$$m_{,r} + mr\frac{\phi_{,r}^2}{n} = \frac{r^n}{n}\left(V + \frac{\phi_{,r}^2}{2}\right), \tag{20b}$$

$$g_{,r} = \frac{r}{n}\phi_{,r}^2. \tag{20c}$$

Eq. (20a) follows from definitions (5) and (15). Equation (20b) is the remaining constraint equation rewritten in terms of the physically interesting mass function m. Our gauge choice is implicitly given by Eq. (20c); it corresponds to the requirement $\dot{g} = 0$ on the initial time slice. The integration is performed numerically using fourth order Runge-Kutta algorithm with constant step size.

Since in asymptotically AdS spacetimes the light rays take finite time to reach spatial infinity and reflect back, the issue of boundary conditions at infinity is a physical one, and cannot be avoided. Various boundary conditions for scalar field ϕ at infinity have been suggested, specifics of which we will discuss later. Additional complication for numerical evolution is that it is unfeasible to include infinity on the grid, so the spacetime has to be cut-off, which we do at a constant (large) radius r_c, and impose boundary conditions for the scalar field there. The remaining boundary condition at the cut-off is the one for the metric coefficient

$$g_{,t} = \frac{\rho_{,xt}}{\rho_{,x}} - \frac{2}{n}\frac{\rho\phi_{,t}\phi_{,x}}{\rho_{,x}}, \tag{21}$$

which follows from the $\{tx\}$ constraint Eq. (13). In the center of the spacetime, one has the usual regularity condition for the scalar field

$$\nabla r \cdot \nabla \phi = 0. \tag{22}$$

The numerical evolution scheme is illustrated in Fig. 2. The field variables are discretized on a square spacetime grid of spacing ϵ. Discretization of the evolution equations is done using the leapfrog scheme, which is second order accurate and nondissipative. In particular, the gradient and box differential operators are discretized as

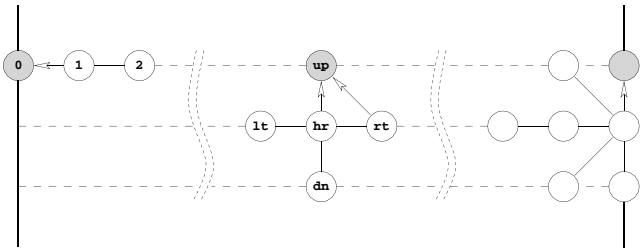

FIG. 2. Numerical evolution scheme.

$$\nabla_x X = \frac{X_{\rm rt} - X_{\rm lt}}{2\epsilon}, \qquad \nabla_t X = \frac{X_{\rm up} - X_{\rm dn}}{2\epsilon}, \tag{23a}$$

$$\Box X = \frac{1}{\epsilon^2}(X_{\rm rt} + X_{\rm lt} - X_{\rm up} - X_{\rm dn}). \tag{23b}$$

Neumann boundary conditions (22) require asymmetric discretization of the derivatives for second order accuracy

$$X'(0) = \frac{1}{2\epsilon}(4X_1 - 3X_0 - X_2). \tag{24}$$

The code was implemented in Fortran, and is efficient enough to run on personal workstation class computers. Since only three subsequent time steps are stored, the code is not memory-limited even for very large grids. All the numerical results presented in this paper were obtained in simulations with the grid size of 65539 points.

IV. COSMIC CENSORSHIP IN STRING THEORY

Hertog, Horowitz, and Maeda argued that cosmic censorship is generically violated in string theory [2]. In their counterexample, they considered $\mathcal{N} = 8$ gauged supergravity in five dimensions, which is thought to be a consistent truncation of ten dimensional type IIB supergravity on S^5. They picked a single scalar component which does not act as a source for any of the other fields, thereby reducing the problem to the one of Einstein gravity in five dimensions minimally coupled to a scalar field ϕ with negative potential

$$V(\phi) = -2e^{2\phi/\sqrt{3}} - 4e^{-\phi/\sqrt{3}}. \tag{25}$$

The potential is unbounded from below, with a maximum value of $V(0) = -6$ which corresponds to the asymptotically AdS spacetime with curvature scale $\ell = 1$. They constructed time-symmetric initial data which has negative reduced mass μ_0 of the initial configuration, namely

$$\phi = \begin{cases} \frac{A}{R_0^2} & r \le R_0 \\ \frac{A}{r^2} & r > R_0 \end{cases}. \tag{26}$$

They further argued that a black hole cannot form in the collapse of this initial configuration (as Schwarzschild-AdS black holes have positive mass), whereas it is possible to show that singularity does form in the collapse of the homogeneous part of the field, and hence concluded

that singularity must be naked and cosmic censorship conjecture is violated.

We use the numerical code described in the previous section to solve Einstein and scalar field equations for the spherically symmetric collapse of the profile (26), and determine the global structure of the resulting spacetime. We find that black holes *do* form in the collapse of initial data (26), contrary to the argument of Hertog *et al.* [2].

We place the spacetime cut-off at $r_c = 25$, which is large enough so that less than 1% of the initial profile mass $\mu_0(\infty)$ lies beyond the cut-off in all cases. At the cut-off, we impose either Dirichlet or Neumann boundary conditions for the scalar field

$$\phi|_{r=r_c} = \text{const}, \qquad \text{[Dirichlet BC]} \tag{27a}$$

$$\partial_r(r^2\phi)|_{r=r_c} = 0, \qquad \text{[Neumann BC]}. \tag{27b}$$

Neumann boundary conditions (27b) correspond to the 'standard' boundary conditions on the fall-off of the scalar field $\phi = \alpha(t)/r^2$ in AdS-CFT correspondence, but are written in this form for computational convenience. We also try alternative suggestion [2] for the initial field profile,

$$\phi = \begin{cases} A\frac{\ln R_0}{R_0^2}, & r \le R_0 \\ A\frac{\ln r}{r^2}, & r > R_0 \end{cases}, \tag{28}$$

which has a slower fall-off rate and much larger negative masses than (26).

Typical spacetime obtained in numerical simulations is shown in Fig. 3. It corresponds to evolution of initial field profile (26) with values of parameters $A = 16$, $R_0 = 4$ ($\phi_0 = 1.0$) subject to Dirichlet boundary conditions (27a). The four panels show density plots of metric coefficients $r(x, t)$ (top left) and $m(x, t)$ (bottom left), as well as the scalar field $\phi(x, t)$ (top right) and its gradient $g^{\mu\nu}\phi_{,\mu}\phi_{,\nu}$ (bottom right). Contours on $r(x, t)$ plot show

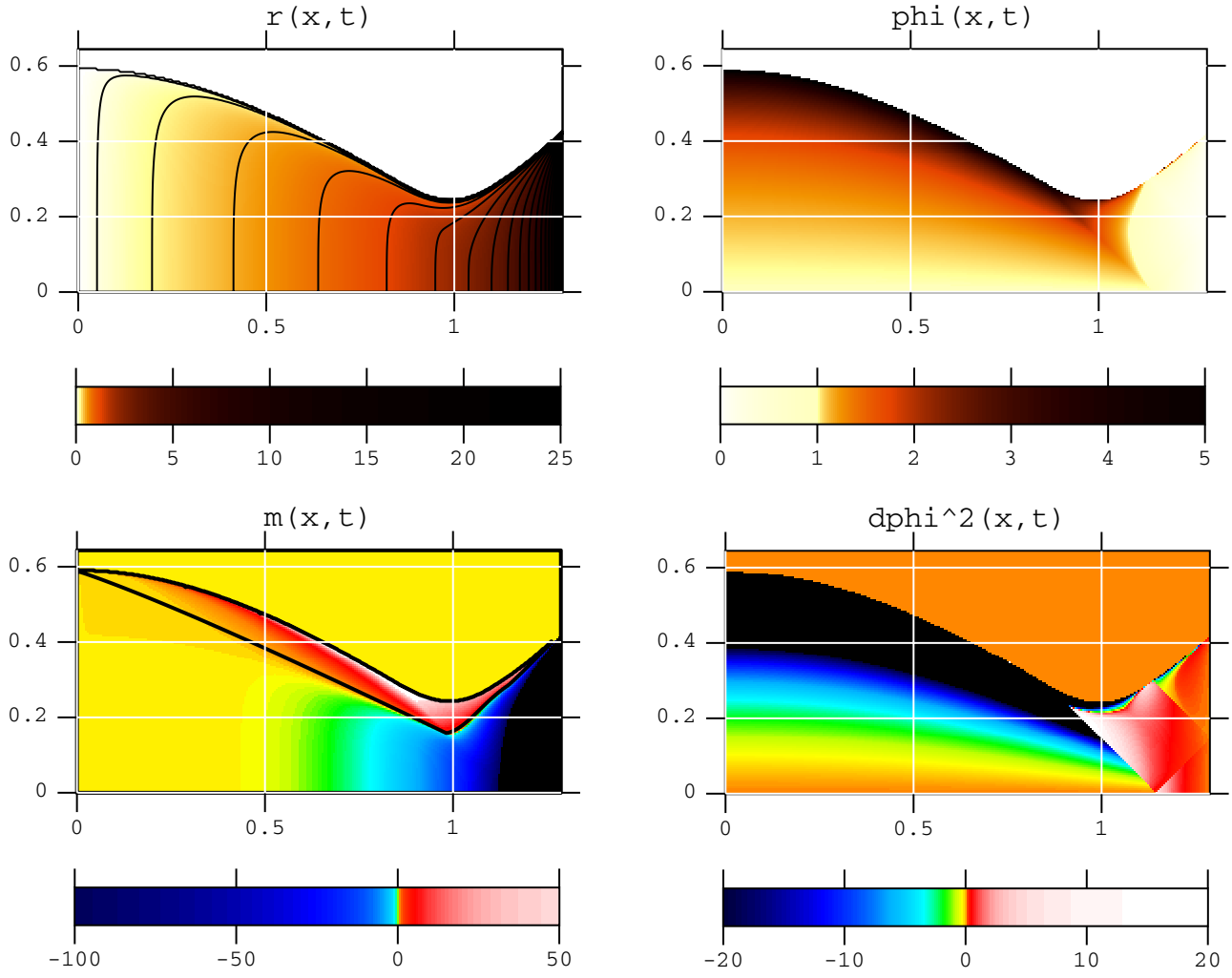

FIG. 3 (color online). Global structure of the spacetime resulting from the evolution of the truncated $1/r^2$ field profile (26) for the values of parameters $A = 16$, $R_0 = 4$. Thick black lines on $m(x, t)$ plot show the locations of the apparent horizon and the singularity.

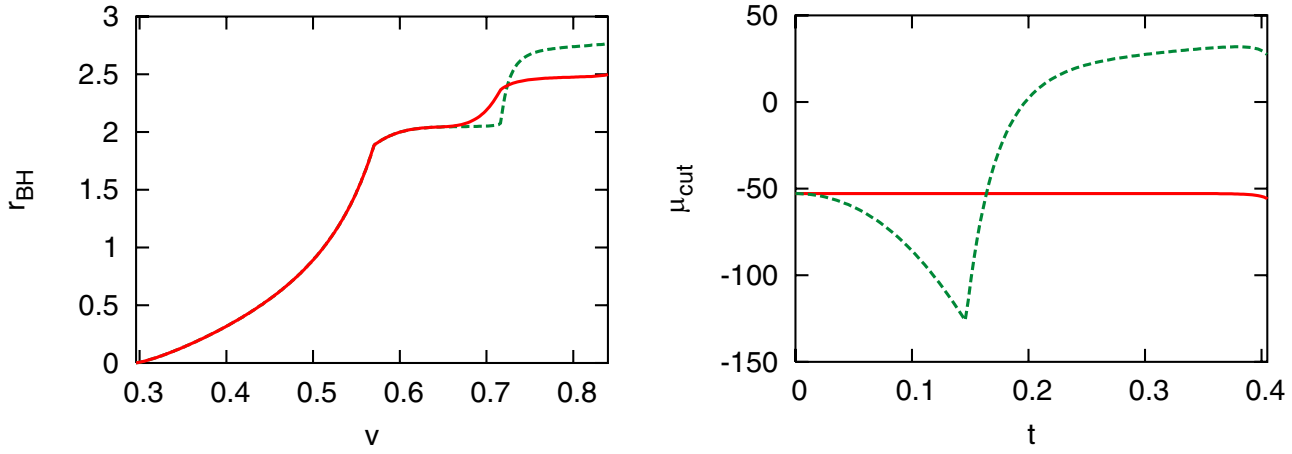

FIG. 4 (color online). The size of the apparent horizon (left) and the reduced mass μ at the cut-off (right) for the same initial conditions as in Fig. 3. Solid and dashed lines show the values corresponding to Dirichlet and Neumann boundary conditions at the cut-off.

isolines of constant radius. The upper thick line on $m(x, t)$ plot is the singularity (where spacetime evolution terminates), while the lower thick line is the apparent horizon (found by condition $f = 0$). Because of our coordinate choice (1), the plots in Fig. 3 essentially are Carter-Penrose conformal diagrams, and show the global structure of the spacetime. It is clear that the black hole has formed in the collapse.

To see if the black hole settles into an almost static configuration or continues to evolve, we plot the size of the apparent horizon $r_{\rm BH}$ as a function of advanced time v in the left panel of Fig. 4. After the stage of growth corresponding to collapse of the homogeneous part of the initial scalar field profile, and sharp steplike increase in size when the outgoing portion of the wavepacket reflects from infinity and falls in (these features in the scalar field profile are most clearly seen in gradient plot in the bottom right of Fig. 3), the black hole settles to almost constant size. The apparent horizon (shown in bottom left panel of Fig. 3) approaches null direction towards the end of the evolution as well, which is consistent with the black hole settling into a static configuration after the formation.

The formation of the black hole does not contradict the negative initial reduced mass μ of the profile. For Dirichlet boundary conditions (27a), the reduced mass at the cut-off is conserved, but the black hole *has scalar hair* which hides the positive black hole mass and makes the total mass at the cut-off negative. No-hair theorems [11,12] do not apply in this case as the cut-off is at a *finite* distance, while the proof of the no-hair theorems involves exclusion of the growing mode at infinity. For Neumann boundary conditions (27b), black holes do not have scalar hair, but the reduced mass at the cut-off *is not conserved*, and grows positive to accommodate the formation of the black hole, as shown in right panel of Fig. 4.

TABLE I. Summary of the numerical results from evolution of the truncated $1/r^2$ (left) and $\ln(r)/r^2$ (right) initial field profiles given by Eqs. (26) and (28) for various values of parameters. Black hole sizes and masses are approximate.

Truncated $1/r^2$ field profile (26)

Initial conditions				Dirichlet BC		Neumann BC		
ϕ_0	A	R_0	μ_0	$r_{\rm BH}$	$\mu_{\rm BH}$	$r_{\rm BH}$	$\mu_{\rm BH}$	$\mu_{\rm cut}$
0.5	2.0	2.0	−0.50	0.86	0.64	0.92	0.78	0.76
1.0	4.0	2.0	−2.42	1.28	2.16	1.40	2.90	2.81
1.5	6.0	2.0	−5.74	1.60	4.56	1.75	6.22	5.88
0.5	4.5	3.0	−3.45	1.33	2.45	1.46	3.34	3.23
1.0	9.0	3.0	−15.58	1.88	8.01	2.08	11.5	11.2
1.5	13.5	3.0	−35.65	2.32	17.2	2.57	25.1	23.5
0.5	8.0	4.0	−11.89	1.78	6.60	1.97	9.47	9.39
1.0	16.0	4.0	−52.78	2.47	21.7	2.74	31.9	31.9
1.5	24.0	4.0	−119.51	3.05	47.9	3.38	71.0	68.0

Truncated $\ln(r)/r^2$ field profile (28)

Initial conditions				Dirichlet BC	
ϕ_0	A	R_0	μ_0	$r_{\rm BH}$	$\mu_{\rm BH}$
0.5	2.885	2.0	−25.1	0.88	0.69
1.0	5.771	2.0	−103.5	1.34	2.51
1.5	8.656	2.0	−238.1	1.57	4.27
0.5	4.096	3.0	−50.2	1.28	2.16
1.0	8.192	3.0	−208.4	1.75	6.22
1.5	12.288	3.0	−479.6	2.02	10.4
0.5	5.771	4.0	−98.6	1.71	5.74
1.0	11.542	4.0	−410.9	2.24	15.1
1.5	17.312	4.0	−945.3	2.56	24.8

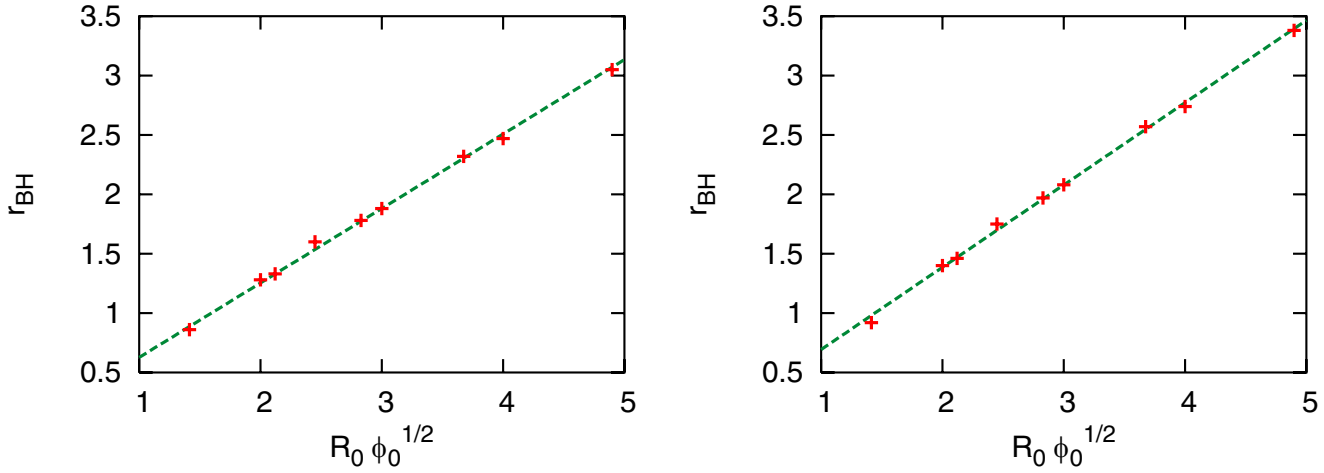

FIG. 5 (color online). The size of the black hole formed in the collapse of the truncated $1/r^2$ field profile (26) as a function of parameters, shown for Dirichlet (left) and Neumann (right) boundary conditions at the cut-off.

In search of violation of cosmic censorship conjecture, we have performed many high-resolution numerical simulations for different initial profiles (26) and (28), different boundary conditions (27a) and (27b) and various values of the parameters ϕ_0 and R_0, but all in vain. In no cases formation of naked singularity was seen. The global structure of the spacetime remains similar to that of Fig. 3, with black holes of various sizes formed in the collapse. Our numerical results are summarized in Table I, which shows sizes and masses of the black holes produced. In addition, the spacetime mass at the cut-off after black hole formation is shown for runs with Neumann boundary conditions. The quoted values should be considered approximate, as the number of useful grid points shrinks near the end of the evolution and precision suffers somewhat (especially for smaller black holes). It is worth noting that the black holes formed in the runs with Neumann boundary conditions indeed have (almost) no-hair, as the masses evaluated at the horizon and at the cut-off are almost the same.

As Fig. 5 shows, the size of a black hole formed in the collapse of the truncated $1/r^2$ field profile (26) scales like $r_{\rm BH} = \alpha R_0 \phi_0^{1/2} = \alpha A^{1/2}$ as a function of profile parameters, with coefficient $\alpha \approx 0.627$ for Dirichlet and $\alpha \approx 0.693$ for Neumann boundary conditions. This agrees well with the lower-bound estimate based on an analysis of the collapse of the homogeneous part of the profile [4]. Although the latter underestimates the value of numerical coefficient (yielding $\alpha = 0.58$), it is only by about 10–20%.

V. CONCLUSION

We have developed a double-null characteristic code implementing N-dimensional spherically symmetric evolution of a minimally coupled scalar field with potential in asymptotically AdS spacetimes, and used it to study the possibility of cosmic censorship violation in string theory. No instances of formation of naked singularity were seen in high-resolution numerical simulations of the evolution of two families of negative mass initial scalar field profiles for various values of parameters and different boundary conditions at the cut-off.

Our results indicate that black holes form and reach steady-state configuration in the collapse, despite the negative initial mass of initial data. Either the spacetime mass becomes positive (for Neumann boundary conditions, where mass μ is not conserved), or the black hole covers itself with negative mass hair (for Dirichlet boundary conditions, where no-hair theorems do not apply because of the finite cut-off), as was pointed out in [4,5].

The possibility of naked singularity formation cannot be ruled out completely by results of numerical simulations, as they only sample a finite number of initial configurations, but in view of the above it seems unlikely. Although no evolutions leading to big crunch were observed from initial configurations considered in this paper, that possibility should be explored further in the future work.

To summarize, the cosmic censorship conjecture was found to hold in all the examples we have studied.

ACKNOWLEDGMENTS

I would like to thank Stephen Shenker, Veronika Hubeny, and Xiao Liu for stimulating discussions. This work was supported by Kavli Institute for Particle Astrophysics and Cosmology and Stanford Institute for Theoretical Physics.

[1] T. Hertog, G. T. Horowitz, and K. Maeda, Phys. Rev. Lett. **92**, 131101 (2004).
[2] T. Hertog, G. T. Horowitz, and K. Maeda, Phys. Rev. D **69**, 105001 (2004).
[3] M. Dafermos, gr-qc/0403033.
[4] V. E. Hubeny, X. Liu, M. Rangamani, and S. Shenker, hep-th/0403198.
[5] M. Gutperle and P. Kraus, J. High Energy Phys. 04 (2004) 024.
[6] D. Garfinkle, Phys. Rev. D **69**, 124017 (2004).
[7] D. Garfinkle, Phys. Rev. D (to be published).
[8] T. Hertog, G. T. Horowitz, and K. Maeda, gr-qc/0405050.
[9] T. Hertog and G. T. Horowitz, J. High Energy Phys. 07 (2004) 073.
[10] A. V. Frolov and U. L. Pen, Phys. Rev. D **68**, 124024 (2003).
[11] J. D. Bekenstein, Phys. Rev. D **51**, 6608 (1995).
[12] K. A. Bronnikov and G. N. Shikin, Gravitation Cosmol. **8**, 107 (2002).